catalysts

MDPI

Communication

Copper-Catalyzed Reaction of *N*-Monosubstituted Hydrazones with CBr_4: Unexpected Fragmentation and Mechanistic Study

Valentine G. Nenajdenko [1], Anna A. Kazakova [2], Alexander S. Novikov [3,*], Namig G. Shikhaliyev [4], Abel M. Maharramov [4], Ayten M. Qajar [4], Gulnar T. Atakishiyeva [4], Aytan A. Niyazova [5], Victor N. Khrustalev [2,6], Alexey V. Shastin [7] and Alexander G. Tskhovrebov [2,*]

1 Department of Chemistry, Lomonosov Moscow State University, Leninskie Gory 1 Bld. 3, 119991 Moscow, Russia
2 Research Institute of Chemistry, Peoples' Friendship University of Russia, 6 Miklukho-Maklaya Street, 117198 Moscow, Russia
3 Institute of Chemistry, Saint Petersburg State University, Universitetskaya Nab, 7/9, 199034 Saint Petersburg, Russia
4 Department of Organic Chemistry, Baku State University, Z. Xalilov 23, 1148 Baku, Azerbaijan
5 Department of Engineering and Applied Sciences, Azerbaijan State University of Economics, M. Mukhtarov 194, 1001 Baku, Azerbaijan
6 Zelinsky Institute of Organic Chemistry RAS, Leninsky Prosp. 47, 119991 Moscow, Russia
7 Institute of Problems of Chemical Physics, Russian Academy of Sciences, 142432 Chernogolovka, Russia
* Correspondence: a.s.novikov@spbu.ru (A.S.N.); tskhovrebov-ag@rudn.ru (A.G.T.)

Abstract: The copper catalyzed reaction of N-monosubstituted hydrazones with carbon tetrabromide leads to formation of expected dibromodiazadienes and unexpected dibromostyrenes. The experimental and theoretical study of the reaction revealed a key role of *N*-centered radicals, which can eliminate aryl radicals to form the corresponding dibromostyrenes. Alternatively, the oxidation of intermediate *N*-centered radicals by Cu(II) results in the corresponding diazadienes. These two reaction pathways are competitive directions of the reaction. Consequently, the reaction can be useful for the synthesis of both dibromostyrenes and rare dibromodiazadienes.

Keywords: azo dyes; radicals; catalysis; DFT; QTAIM; noncovalent interactions; halogen bonding

Citation: Nenajdenko, V.G.; Kazakova, A.A.; Novikov, A.S.; Shikhaliyev, N.G.; Maharramov, A.M.; Qajar, A.M.; Atakishiyeva, G.T.; Niyazova, A.A.; Khrustalev, V.N.; Shastin, A.V.; et al. Copper-Catalyzed Reaction of *N*-Monosubstituted Hydrazones with CBr_4: Unexpected Fragmentation and Mechanistic Study. *Catalysts* **2023**, *13*, 1194. https://doi.org/10.3390/catal13081194

Academic Editor: Hiroto Yoshida

Received: 27 July 2023
Revised: 8 August 2023
Accepted: 8 August 2023
Published: 9 August 2023

1. Introduction

Hydrazones are versatile synthons employed in organic chemistry. Recently, Nenajdenko et al. have discovered novel copper-mediated reactions of *N*-unsubstituted hydrazones with polyhalogenated compounds [1]. As a result, a new general method for the synthesis of various alkenes has been created [2–6]. This approach can be used for the preparation of valuable catalysts [7] or azo dyes [8]. Azo dyes are important organic compounds containing the structural element R–N=N–R', which exhibits diverse applications in various fields. These applications include their use as sensors, ligands, liquid crystals, optical data storage media, nonlinear optic materials, dye-sensitized solar cells, color-changing substances, molecular switches, and more [9–11]. The specific properties of azo dyes mentioned above are significantly influenced by the functional groups attached to the –N=N– structural unit.

Importantly, the *N*-substitution of hydrazones had a dramatic impact on the reaction outcome. For instance, the copper-mediated reaction of monosubstituted hydrazones **1** with carbon tetrachloride resulted in the formation of the corresponding diazabutadienes **2** (Scheme 1) [1]. The mechanism of this reaction includes participation of short-lived radical species, the reaction path of which has been confirmed using various radical traps.

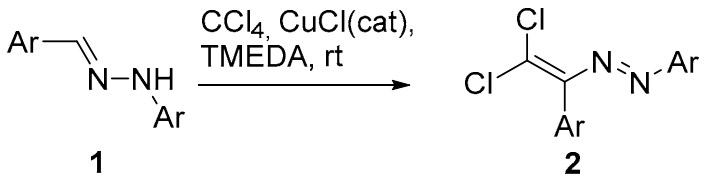

Scheme 1. Synthesis of dichlorodiazadienes.

Excited by this discovery, we decided to systematically investigate the Cu-catalyzed reactions of *N*-monosubstituted hydrazones with polyhalogenated compounds. Surprisingly, we found that the action of CBr_4 on the *N*-monosubstituted hydrazones results in the formation of the dibromoalkene in addition to the expected dibromodiazabutadienes. This study is devoted to the investigation of the mechanism of the reaction with CBr_4. It was studied theoretically by DFT calculations; moreover, some additional experiments revealed the features of the reaction.

2. Results and Discussion

Initially, we aimed to prepare dibromodiazadienes and further explore their reactivity in the analogous fashion as we did for dichloro derivatives [2,7,12–15]. The starting N-monosubstituted hydrazones were synthesized by the condensation of hydrazines with the corresponding aldehydes. The addition of the excess of CBr_4 to hydrazones in the presence of the catalytic amount of CuCl in DMSO resulted in a gradual orange coloration of the mixture and noticeable gas bubbling (presumably N_2 exrusion). The analysis of the reaction mixture indicated the formation of expected dibromodiazadienes (Scheme 2). However, in addition to dibromodiazadienes, we observed the formation of unexpected dibromoalkenes in significant yields (Scheme 2, synthetic part). It should be noted that the reaction with CCl_4 did not result in the formation of analogous dichloroalkenes in any noticeable amounts. That means that fragmentation takes place in the case of the reaction with carbon tetrabromide and the C–N bond is broken during the reaction.

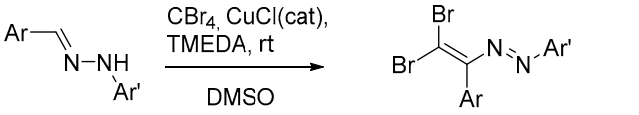

	Ar	Ar'	Yield
7	*p*-tolyl	Ph	52%
8	*p*-tolyl	*p*-tolyl	60%
9	*p*-tolyl	*p*-ClC_6H_4	51%
10	*p*-tolyl	*p*-CNC_6H_4	56%
11	*p*-tolyl	*p*-$NO_2C_6H_4$	48%
12	*p*-tolyl	*p*-BrC_6H_4	56%
13	*p*-PhC_6H_4	Ph	10%

	Ar	Yield
7a	*p*-tolyl	22%
8a	*p*-tolyl	20%
9a	*p*-tolyl	17%
10a	*p*-tolyl	19%
11a	*p*-tolyl	24%
12a	*p*-tolyl	20%
13a	*p*-PhC_6H_4	56%

Scheme 2. Cu-mediated reaction between hydrazones and CBr_4.

Previously, we proposed the mechanism of the reaction of N-substituted hydrazones **1** with CCl_4 [1]. It includes the addition of the trichloromethyl radical to hydrazone followed by oxidation of the intermediate N-centered radical **D**. This oxidation leads to the formation of azo-compound **E**. The subsequent base-induced elimination of HCl gives the final dichlorodiazadiene **2**. Having observed unexpected fragmentation in the case of the reaction with carbon tetrabromide, we proposed that the reason for the observed fragmentation is connected with the transformation of intermediate **D**. Our idea is connected to the elimination of the aryl radical from **D** to form azene intermediate, which, in turn, is transformed into dibromostyrene (Scheme 3).

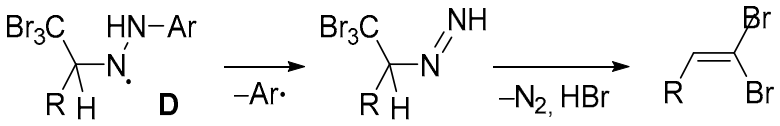

Scheme 3. Plausible route to dibromostyrene via aryl radical elimination.

First, we performed some model experiments with hydrazones derived from p-cyanophenyl hydrazine and p-bromophenyl hydrazine. GC-MS analyses of the reaction mixtures for **10** and **12** showed the formation of significant amounts of benzonitrile and p-bromobenzonitrile and bromobenzene and p-dibromobenzene, correspondingly. These data indirectly indicated on the generation of the corresponding p-cyanophenyl and p-bromophenyl radicals in the course of the reactions, which abstract either hydrogen or bromine atoms to furnish the final arenes. Most probably, observation of two pathways for transformation of arylradicals can be explained in the frames of their stability and lifetime. It should be noted that relevant chemistries have been observed before [16–18].

In order to obtain more insight into the reaction mechanism, we performed DFT calculation of the Cu-mediated reaction between hydrazones and CCl_4 or CBr_4. The plausible mechanism for catalytic cycle is depicted in Scheme 4.

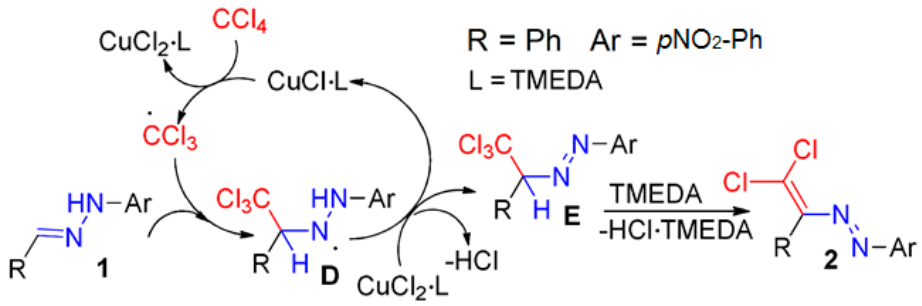

Scheme 4. Schematic representation of elementary steps for theoretically studied plausible model catalytic cycle involving reaction system with chlorine-containing species (in case of CBr_4-based reaction system all transformations are the same).

The results of DFT calculations (in dimethyl sulfoxide continuum solvation model) reveal the following: (a) in the very first step of catalytic cycle, formation of $CCl_3\cdot$ is only slightly endergonic (0.1 kcal/mol in terms of Gibbs free energies), whereas formation of $CBr_3\cdot$ is much more thermodynamically unfavorable (8.5 kcal/mol in terms of Gibbs free energies); (b) the second step of the catalytic cycle (attack of C=N bond in hydrazone **1** by $CX_3\cdot$, X = Cl, Br) is much more energetically profitable in the case of $CBr_3\cdot$ (viz −20.0 kcal/mol in terms of summary Gibbs free energies compare with −10.2 kcal/mol in case of $CCl_3\cdot$); (c) the last step of the catalytic cycle resulting in formation of diazene **E** is endergonic in both cases, but in the case of a reaction system with chlorine-containing species—in a lesser degree compared with the reaction system based on bromine-containing substances; (d) in case of the CBr_4-based reaction system, overall thermodynamic favorability of three stages of catalytic cycle (viz. CuX_TMEDA + CX_4 → CuX_2_TMEDA + $CX_3\cdot$, $CX_3\cdot$ + 1 → D·_X, and D·_X + CuX_2_TMEDA → CuX_TMEDA + HX + E_X; X = Cl, Br) is −7.7 kcal/mol in terms of Gibbs free energies vs. −2.9 kcal/mol in case of CCl_4-based reaction system; and (e) the subsequent TMEDA-assisted elimination of HCl/HBr molecule from **E** furnishes the reaction product 1,2-diaza-1,3-diene **2**, which is highly exergonic in both cases. We also considered some other alternative pathways for the formation of dichaloalkenes, but they all are very energetically unfavorable (Table 1).

Table 1. Calculated values of total electronic energies, enthalpies, and Gibbs free energies of reaction (ΔE, ΔH, and ΔG in kcal/mol) for elementary steps of model catalytic cycle.

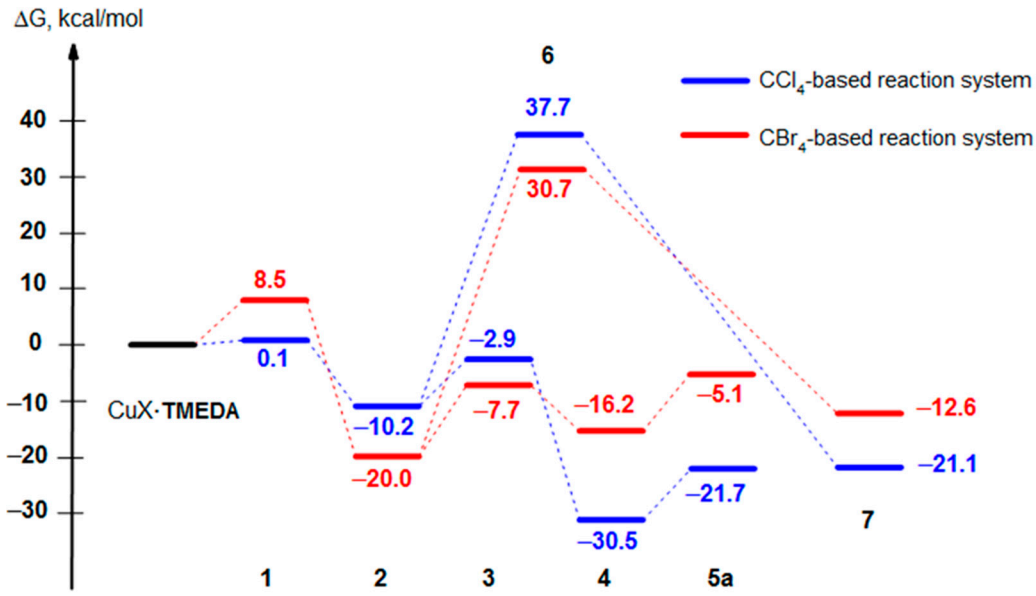

Elementary Step	ΔE	ΔH	ΔG
CCl_4-based reaction system			
CuCl_TMEDA + CCl_4 → $CuCl_2$_TMEDA + CCl_3· (1)	1.4	1.9	0.1
CCl_3· + 1 → D·_Cl (2)	−27.0	−24.7	−10.3
D·_Cl + $CuCl_2$_TMEDA → CuCl_TMEDA + HCl + E_Cl (3)	22.3	18.5	7.3
E_Cl + TMEDA → H-TMEDA$^+$ + Cl^- + 2_Cl (4)	−20.2	−18.1	−27.6
2_Cl + HCl → Cl_2C=CHPh + Cl^- + PhN=N^+ (5a)	17.8	19.0	8.8
2_Cl + HCl → Cl_2C=CHPh + PhN=N^+···Cl^- (5b)	12.9	14.3	9.8
2_Cl + H-TMEDA$^+$ → Cl_2C=CHPh + TMEDA + PhN=N^+ (5c)	48.7	44.2	32.1
F_Cl_cis → F_Cl_trans	−3.4	−3.1	−3.2
D·_Cl → F_Cl_trans + Ph· (6)	63.7	61.2	47.9
F_Cl_trans → HCl + N_2 + Cl_2C=CHPh (7)	−31.8	−37.0	−58.8
CBr_4-based reaction system			
CuBr_TMEDA + CBr_4 → $CuBr_2$_TMEDA + CBr_3· (1)	8.8	9.6	8.5
CBr_3· + 1 → D·_Br (2)	−45.6	−43.1	−28.5
D·_Br + $CuBr_2$_TMEDA → CuBr_TMEDA + HBr + E_Br (3)	28.2	23.4	12.3
E_Br + TMEDA → H-TMEDA$^+$ + Br^- + 2_Br (4)	−3.9	−0.9	−8.5
cis-PhN=N–Br → *trans*-PhN=N–Br	2.5	2.7	2.9
2_Br + HBr → Br_2C=CHPh + *cis*-PhN=N–Br (5a)	13.9	14.7	11.1
2_Br + HBr → Br_2C=CHPh + Br^- + PhN=N^+ (5a′)	29.0	30.0	18.3
2_Br + HBr → Br_2C=CHPh + PhN=N^+···Br^- (5b)	14.6	16.8	12.0
2_Br + H-TMEDA$^+$ → Br_2C=CHPh + TMEDA + PhN=N^+ (5c)	56.2	51.1	37.4
F_Br_cis → F_Br_trans	−3.5	−3.4	−3.5
D·_Br → F_Br_trans + Ph· (6)	66.4	63.8	50.7
F_Br_trans → HBr + N_2 + Br_2C=CHPh (7)	−14.9	−20.5	−43.3

As a result, we propose modification of the previous mechanism of the reaction, which can explain the formation of either azadienes or alkenes. The key steps of this radical reaction are the same as those given in Scheme 4. However, one important modification is elimination of aryl radical from the intermediate **D** to form the corresponding azene **F**. Finally, base-induced elimination in this case leads to formation of the corresponding dibromo-alkene (Scheme 5).

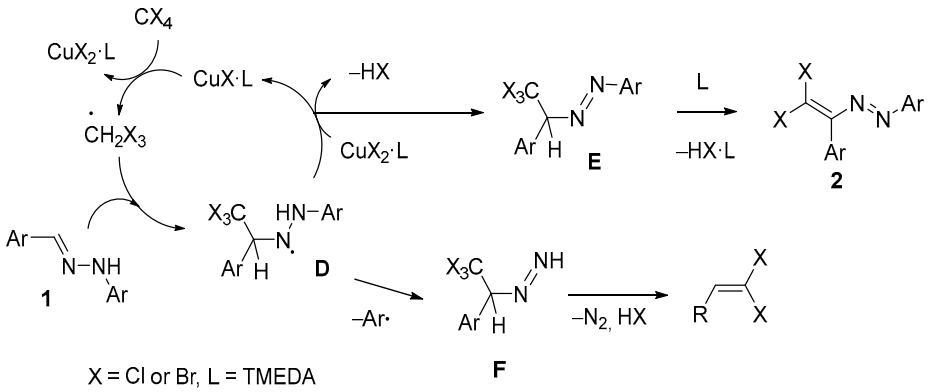

Scheme 5. Proposed mechanism for all observed transformations in the studied reaction system.

Compounds **13** and **13a** could be recrystallized from CH_2Cl_2 to produce a single crystal suitable for the X-ray analysis (Figure 1).

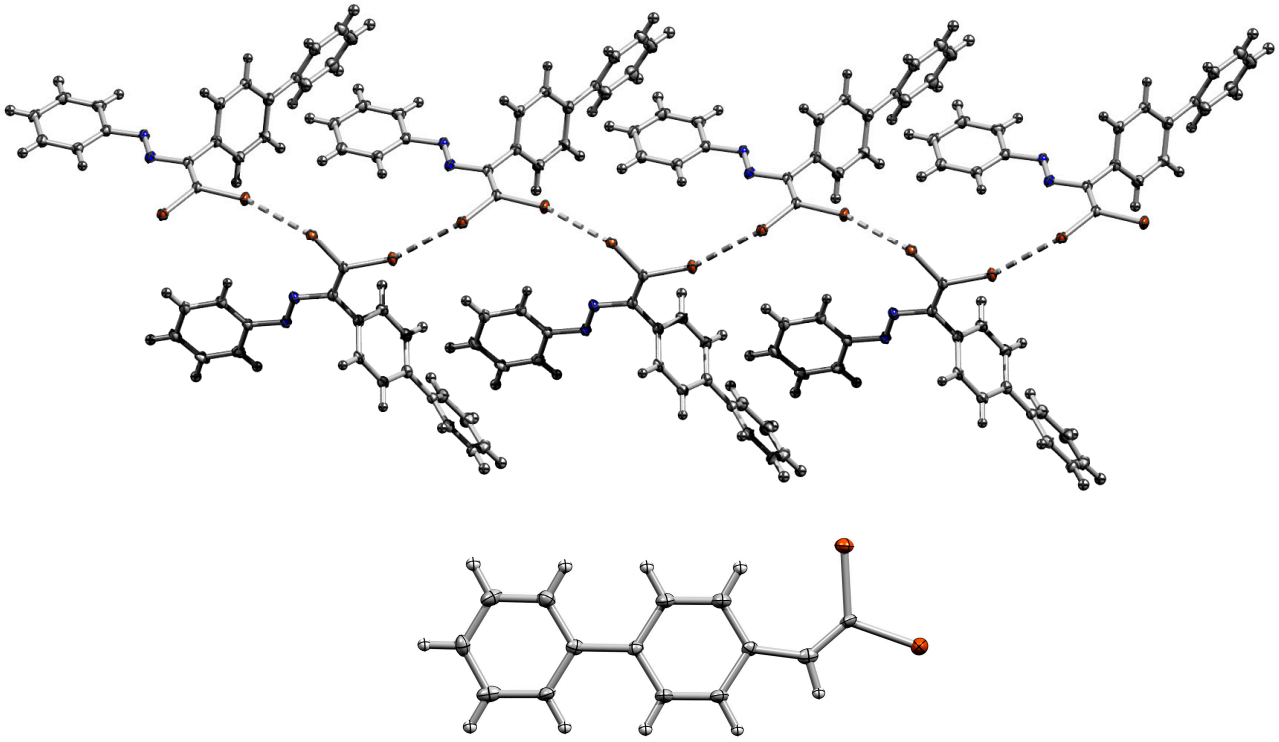

Figure 1. Molecular structures of **13** (**top**) and **13a** (**bottom**) in the crystal. Thermal ellipsoids are at 50% probability. Blue, brown, gray and light gray ellipsoids represent nitrogen, bromine, carbon and hydrogen atoms, respectively.

Interestingly, **13** featured intermolecular halogen bonding Br···Br (3.435 Å, 94% of Bondi's vdW radii sum for two bromine atoms [19–21], Figure 2) in the solid state, whereas such noncovalent contacts are absent in the X-ray structure of **13a**. It should be noted that we demonstrated earlier that highly polarizable dichlorodiazadienes are good sigma-hole donors [12–15].

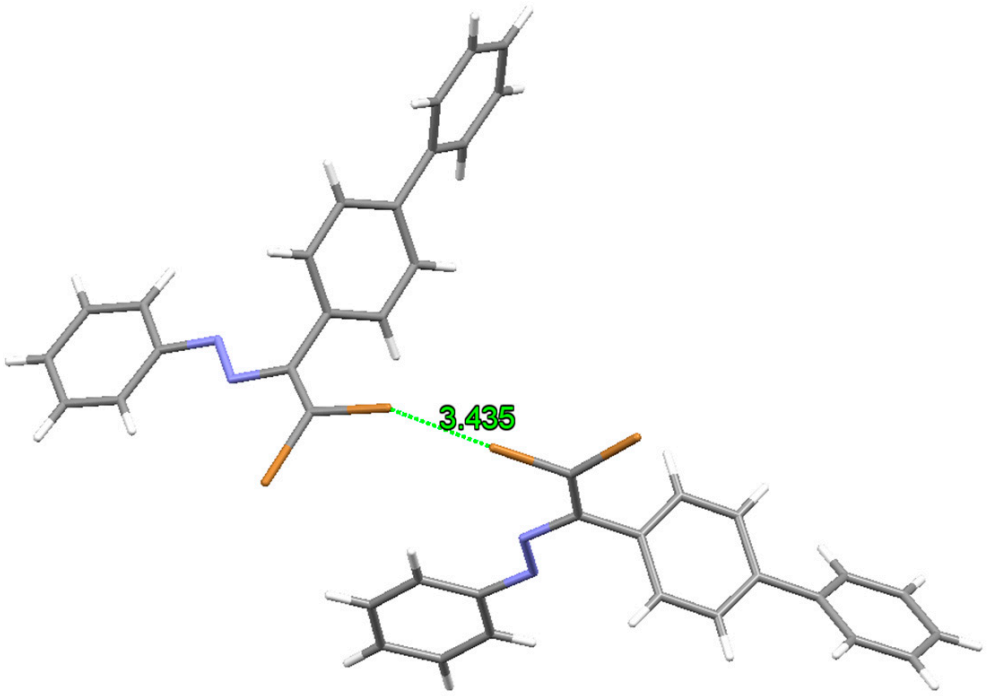

Figure 2. Intermolecular halogen bonding Br···Br in the crystal structure of **13**.

To deeper explore these noncovalent interactions in **13**, we carried out a theoretical topological analysis of the electron density distribution within the QTAIM approach [22] for model supramolecular associate (appropriate xyz-file with Cartesian atomic coordinates is given in Supplementary Materials). The QTAIM analysis demonstrates the presence of bond critical point (3, −1) (BCP) for halogen bonding Br···Br in the model supramolecular associate under study. The low magnitude of the electron density (0.009 a.u.), positive value of the Laplacian of electron density (0.032 a.u.), and close to zero positive energy density (0.002 a.u.: Lagrangian kinetic energy G(r) = 0.006 a.u. and potential energy density V(r) = −0.004 a.u.) in this BCP, as well as the estimated strength for appropriate contact (1.5 kcal/mol, $E_{int} \approx 0.58(-V(r))$ [23], this empirical correlation was developed exclusively for noncovalent interactions involving bromine atoms) are typical for halogen bonds [21,24–28]. The contour line diagram of the Laplacian of electron-density distribution $\nabla^2\rho(r)$, bond paths, and selected zero-flux surfaces, visualization of electron localization function (ELF) and reduced-density gradient (RDG) analyses for halogen bonding Br···Br in the model supramolecular associate based on the experimental X-ray structure **13** are shown in Figure 3.

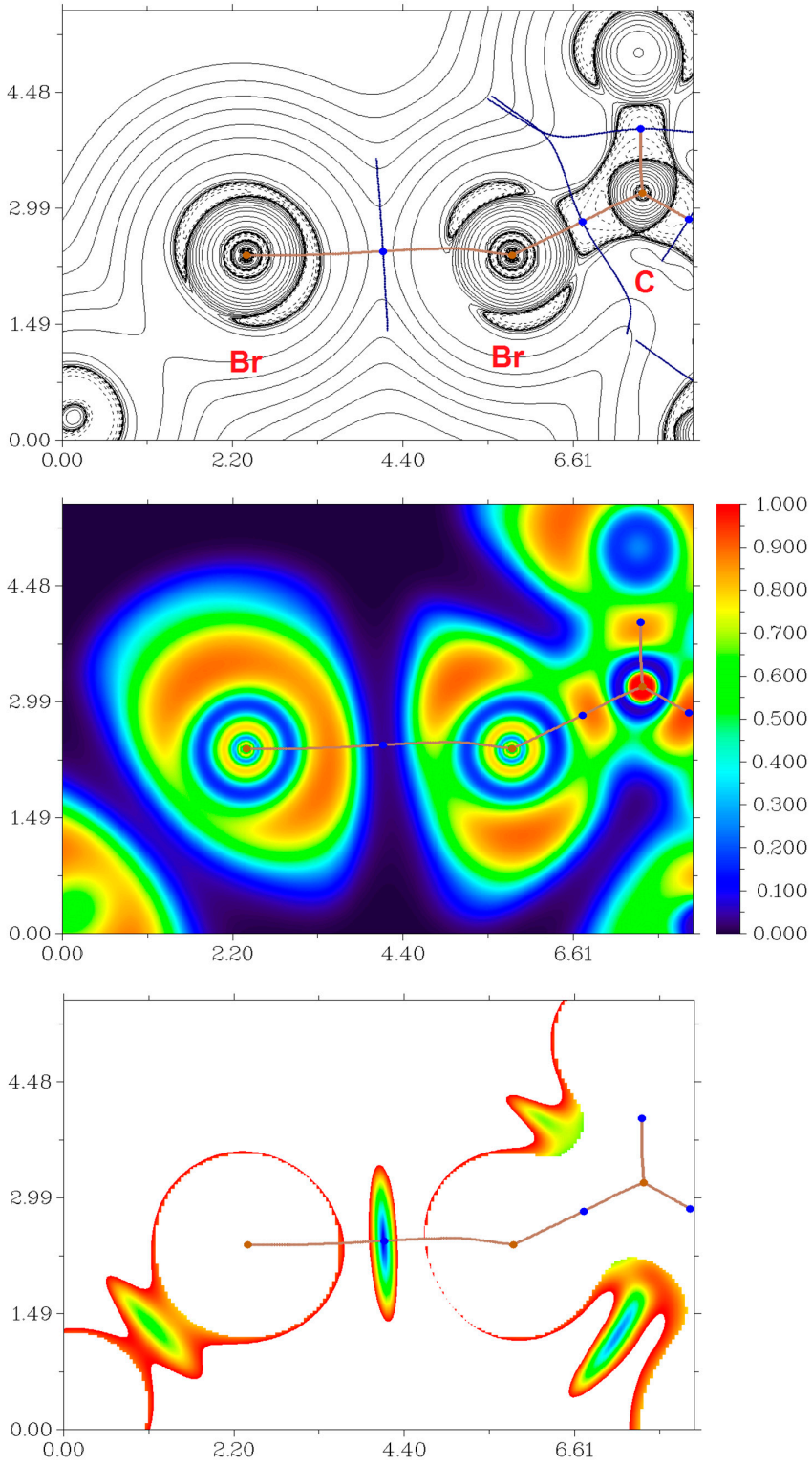

Figure 3. Contour line diagram of the Laplacian of electron density distribution $\nabla^2\rho(\mathbf{r})$, bond paths, and selected zero-flux surfaces (**top panel**), visualization of electron localization function (ELF, **center panel**) and reduced density gradient (RDG, **bottom panel**) analyses for halogen bonding Br···Br in the model supramolecular associate based on the experimental X-ray structure **13**. Bond critical points (3, −1) are shown in blue, nuclear critical points (3, −3)—in pale brown, bond paths are shown as pale brown lines, length units—Å, and the color scale for the ELF and RDG maps is presented in a.u.

3. Materials and Methods

General remarks: Unless stated otherwise, all the reagents used in this study were obtained from commercial sources (Aldrich, TCI-Europe, Strem, ABCR). NMR spectra were recorded on a L. Krause.

Avance 300 (^{1}H: 300 MHz, Karlsruhe, Germany); and chemical shifts (δ) are given in ppm relative to TMS, coupling constants (J) in Hz. Solvents were purified by distillation over the indicated drying agents and were transferred under Ar: Et_2O (Mg/anthracene), CH_2Cl_2 (CaH_2), and hexane (Na/K). Flash chromatography: Merck Geduran® Si 60 (Darmstadt, Germany) (40–63 μm).

Computational details: The full geometry optimization of all model structures and single point calculations based on the experimental X-ray geometry of **13** were carried out at the DFT level of theory using the dispersion-corrected hybrid functional ωB97XD [29] with the help of the Gaussian-09 program package [30]. The standard 6-31+G* basis sets were used. No symmetry restrictions were applied during the geometry optimizations. The solvent effects were taken into account using the SMD (Solvation Model based on Density) continuum solvation model suggested by Truhlar and coworkers [31] for dimethyl sulfoxide. The Hessian matrices were calculated analytically for all optimized model structures to prove the location of the correct minimum on the potential energy surface (no imaginary frequencies were found in all cases) and to estimate thermodynamic parameters at 25 °C and 1 atm. The topological analysis of the electron density distribution has been performed by using the Multiwfn program (version 3.7) [32]. The Cartesian atomic coordinates for all model structures are presented in xyz-files (Supplementary Materials).

Schiff bases **1**–**6** were synthesized according to the following method (similar procedures for the synthesis of hydrazones were reported earlier) [13–15,33–39]. A mixture of a corresponding hydrazine (10.2 mmol), CH_3COONa (0.82 g) and *p*-bromobenzaldehyde (10 mmol) were refluxed with stirring in ethanol (50 mL) for 2 h. The reaction mixture was cooled to room temperature and water (50 mL) was added to give a precipitate of crude product, which was filtered off, washed with diluted ethanol (1:1 with water) and dried in vacuo.

1. (E)-1-(4-methylbenzylidene)-2-phenylhydrazine. white solid (82%), mp 175 °C. ^{1}H NMR (300 MHz, DMSO-d_6) δ 10.27 (s, 1H, –NH), 7.84 (s, 1H, –CH), 7.54 (d, *J* = 7.4 Hz, 2H, arom), 7.20 (d, *J* = 7.2 Hz, 4H, arom), 7.07 (d, *J* = 7.5 Hz, 2H, arom), 6.73 (t, *J* = 7.4 Hz, 1H, arom), 2.31 (s, 3H, –CH_3). ^{13}C NMR (75 MHz, DMSO) δ 145.8, 137.8, 137.0, 133.5, 129.7, 129.5, 126.05, 118.9, 112.3, 21.3.

2. (E)-1-(4-methylbenzylidene)-2-(p-tolyl)hydrazine. white solid (87%), mp 152 °C. ^{1}H NMR (300 MHz, DMSO-d_6) δ 10.15 (s, 1H, –NH), 7.80 (s, 1H, –CH), 7.52 (d, *J* = 7.4 Hz, 2H, arom), 7.18 (d, *J* = 7.4 Hz, 2H, arom), 7.00 (q, *J* = 7.8 Hz, 4H, arom), 2.30 (s, 3H, –CH_3), 2.21 (s, 3H, –CH_3). ^{13}C NMR (75 MHz, DMSO) δ 143.6, 137.6, 136.3, 133.6, 129.9, 129.6, 127.4, 125.9, 112.3, 21.3, 20.7.

3. (E)-1-(4-CHlorophenyl)-2-(4-methylbenzylidene)hydrazine. Yellow solid (70%), mp 155 °C. ^{1}H NMR (300 MHz, DMSO-d_6) δ 10.42 (s, 1H, –NH), 7.88 (s, 1H, –CH), 7.55 (s, 2H, arom), 7.41–6.95 (m, 6H, arom), 2.29 (s, 3H, –CH_3). ^{13}C NMR (75 MHz, DMSO) δ 144.8, 138.0, 137.9, 133.35, 129.6, 129.3, 126.1, 122.3, 113.7, 21.3.

4. (E)-4-(2-(4-methylbenzylidene)hydrazinyl)benzonitrile. White solid (67%), mp 178 °C. ^{1}H NMR (300 MHz, DMSO-d_6) δ 10.89 (s, 1H, –NH), 7.94 (s, 1H, –CH), 7.68–7.50 (m, 5H, arom), 7.18 (dd, *J* = 26.3, 7.6 Hz, 5H, arom), 2.32 (s, 3H, –CH_3). ^{13}C NMR (75 MHz, DMSO) δ 140.6, 138.9, 134.1, 132.7, 132.2, 129.8, 126.6, 120.6, 116.5, 112.4, 21.4.

5. (E)-1-(4-methylbenzylidene)-2-(4-nitrophenyl)hydrazine. red solid (79%), mp 168 °C. ^{1}H NMR (300 MHz, DMSO-d_6) δ 11.24 (s, 1H, –NH), 8.12 (d, *J* = 8.9 Hz, 2H, arom), 8.01 (s, 1H, –CH), 7.62 (d, *J* = 7.8 Hz, 2H, arom), 7.24 (d, *J* = 7.8 Hz, 2H, arom), 7.15 (d, *J* = 8.5 Hz, 2H, arom), 2.32 (s, 3H, –CH_3). ^{13}C NMR (75 MHz, DMSO) δ 150.0, 141.4, 138.4, 137.6, 131.4, 128.8, 125.9, 125.6, 110.5, 20.4.

6. (E)-1-(4-bromophenyl)-2-(4-methylbenzylidene)hydrazine white solid (72%), mp 181 °C. ^{1}H NMR (300 MHz, DMSO-d_6) δ 10.40 (s, 1H, –NH), 7.84 (s, 1H, –CH), 7.54 (d,

J = 8.0 Hz, 2H, arom), 7.35 (d, *J* = 8.8 Hz, 2H, arom), 7.20 (d, *J* = 7.9 Hz, 2H, arom), 7.01 (d, *J* = 8.8 Hz, 2H, arom), 2.31 (s, 3H, $-CH_3$). ^{13}C NMR (75 MHz, DMSO) δ 145.1, 138.1, 138.0, 133.2, 132.1, 129.72, 126.2, 114.2, 109.7, 21.3.

Synthesis of dibromodiazadiens.

A 20 mL screw neck vial was charged with DMSO (10 mL), **1**–**7** (1 mmol), tetramethylethylenediamine (TMEDA) (295 mg, 2.5 mmol), CuCl (2 mg, 0.02 mmol) and CBr_4 (1 mmol). After 1–3 h (until TLC analysis showed complete consumption of corresponding Schiff base), the reaction mixture was poured into ~0.01 M solution of HCl (100 mL, ~pH = 2), and extracted with dichloromethane (3 × 20 mL). The combined organic phase was washed with water (3 × 50 mL), brine (30 mL), dried over anhydrous Na_2SO_4 and concentrated in vacuo. The residue was purified by column chromatography on silica gel using appropriate mixtures of hexane and dichloromethane (3/1–1/1).

7. (E)-1-(2,2-dibromo-1-(p-tolyl)vinyl)-2-phenyldiazene. Red solid (52%), mp 125 °C. ^1H NMR (300 MHz, Chloroform-*d*) δ 7.85–7.77 (m, 2H, arom), 7.46 (d, *J* = 5.2 Hz, 3H, arom), 7.25 (s, 1H, arom), 7.09 (d, *J* = 7.9 Hz, 2H, arom), 2.43 (s, 3H, $-CH_3$). ^{13}C NMR (75 MHz, $CDCl_3$) δ 156.4, 152.9, 138.5, 131.5, 131.2, 129.6, 129.0, 128.9, 123.3, 21.5.

7a. 1-(2,2-dibromovinyl)-4-methylbenzene. mp 115 °C, (22%). ^1H NMR (300 MHz, DMSO-d_6) δ 7.68 (s, 1H, -vinyl H), 7.48 (d, *J* = 8.0 Hz, 2H, arom), 7.19 (d, *J* = 7.9 Hz, 2H, arom), 2.28 (s, 3H, $-CH_3$). ^{13}C NMR (75 MHz, DMSO) δ 138.8, 137.2, 132.5, 129.4, 128.6, 88.5, 21.4. The spectra of a given compound overlaps with those of the literature [40].

1H NMR (400 MHz, CDCl3) δ = 7.44 (s,1H), 7.43 (d, *J* = 6.7 Hz, 2H), 7.17 (d, *J* = 7.5 Hz, 2H), 2.34 (s, 3H); ^{13}C NMR (100 MHz, CDCl3) δ = 138.8, 136.9, 132.6, 129.2, 128.5, 88.7, 21.5.

8. (E)-1-(2,2-dibromo-1-(p-tolyl)vinyl)-2-(p-tolyl)diazene. red solid (60%), mp 117 °C. ^1H NMR (300 MHz, Chloroform-*d*) δ 7.82–7.73 (m, 2H, arom), 7.33–7.25 (m, 4H, arom), 7.13 (d, *J* = 8.0 Hz, 2H, arom), 2.45 (d, *J* = 7.5 Hz, 6H, $-CH_3$). ^{13}C NMR (75 MHz, $CDCl_3$) δ 131.4, 130.9, 129.8, 129.7, 129.3, 129.2, 128.9, 128.4, 123.4, 122.9, 21.7, 21.0.

7a. (Twenty-one percent)

9. (E)-1-(4-chlorophenyl)-2-(2,2-dibromo-1-(p-tolyl)vinyl) diazene. red solid (51%), mp 132 °C. ^1H NMR (300 MHz, Chloroform-*d*) δ 7.75 (d, *J* = 8.2 Hz, 2H, arom), 7.41 (d, *J* = 8.4 Hz, 2H, arom), 7.25 (d, *J* = 8.1 Hz, 2H, arom), 7.05 (d, *J* = 7.6 Hz, 2H, arom), 2.42 (s, 3H, $-CH_3$). ^{13}C NMR (75 MHz, $CDCl_3$) δ 135.3, 135.0, 134.6, 131.3, 131.1, 129.5, 129.3, 128.9, 125.4, 124.5, 30.99

7a. (Seventeen percent)

10. (E)-4-((2,2-dibromo-1-(p-tolyl)vinyl)diazenyl)benzonit-rile. yellow solid (56%), mp 142 °C. ^1H NMR (300 MHz, Chloroform-*d*) δ 7.70–7.62 (m, 4H, arom), 7.54 (d, *J* = 8.6 Hz, 4H, arom), 1.27 (s, 3H, $-CH_3$). ^{13}C NMR (75 MHz, $CDCl_3$) δ 142.9, 138.5, 136.8, 133.4, 132.6, 128.0, 123.8, 118.0, 113.0, 111.2, 100.5, 29.7.

7a. (Twenty-one percent)

11. (E)-1-(2,2-dibromo-1-(p-tolyl)vinyl)-2-(4-nitrophenyl) diazene. red solid (48%), mp 184 °C. ^1H NMR (300 MHz, Chloroform-*d*) δ 8.41 (s, 1H, arom), 8.23 (d, *J* = 7.4 Hz, 2H, arom), 7.92–7.73 (m, 2H, arom), 7.27–7.21 (m, 3H, arom), 2.43 (s, 3H, $-CH_3$). ^{13}C NMR (75 MHz, $CDCl_3$) δ 129.7, 129.3, 128.0, 126.8, 126.1, 124.6, 123.4, 114.5, 112.8, 112.6, 21.3.

7a. (Twenty-four percent)

12. (E)-1-(4-bromophenyl)-2-(2,2-dibromo-1-(p-tolyl)vinyl) diazene. red solid (56%), mp 110 °C. ^1H NMR (300 MHz, Chloroform-*d*) δ 7.67 (d, *J* = 8.7 Hz, 2H, arom), 7.57 (d, *J* = 8.8 Hz, 2H, arom), 7.24 (d, *J* = 8.0 Hz, 2H, arom), 7.05 (d, *J* = 8.0 Hz, 2H, arom), 2.41 (s, 3H, $-CH_3$). ^{13}C NMR (75 MHz, $CDCl_3$) δ 151.6, 138.7, 132.3, 131.3, 130.9, 129.5, 128.9, 126.1, 124.7, 111.1, 21.4.

7a. (Twenty percent)

13. Orange solid (10%). ^1H NMR (700 MHz, DMSO-*d6*) *δ* 6.90–6.84 (m, 6H, H^3, H^6 and H^7), 6.71–6.65 (m, 3H, H^{13} and H^{14}), 6.62 (t, *J* = 7.7 Hz, 2H, H^2), 6.53 (t, *J* = 7.4 Hz, 1H, H^1), 6.43 (d, *J* = 8.3 Hz, 2H, H^{12}); ^{13}C NMR (176 MHz, DMSO-d_6) *δ* 156.3, 152.7, 140.8, 139.9, 133.6, 132.7, 130.8, 130.1, 129.5, 128.3, 127.2, 127.0, 123.3, 112.2.

13a. 4-(2,2-dibromovinyl)-1,1′-biphenyl. Colorless solid (56%). Analytical data were in accord with the literature [41].

4. Conclusions

In this work, we demonstrated that the Cu-catalyzed reaction between CBr_4 and the *N*-monosubstituted hydrazones results in the formation of corresponding mixtures of dibromodiazabutadienes and dibromoalkenes. The mechanism was investigated, and the results indicated on the generation of aryl radicals over the course of the hydrazone fragmentation. Overall, the reaction can be useful for the synthesis of both dibromosyrenes and rare dibromodiazadienes.

Supplementary Materials: The following supporting information can be downloaded at: https://www.mdpi.com/article/10.3390/catal13081194/s1, Table S1: Calculated total electronic energies (E, in Hartree), enthalpies (H, in Hartree), Gibbs free energies (G, in Hartree), and entropies (S, cal/mol·K) for optimized equilibrium model structures; Table S2: Crystal data and structure refinement for the compounds studied [42–44].

Author Contributions: Conceptualization, V.G.N. and A.G.T.; investigation, A.A.K., N.G.S., G.T.A., A.A.N., V.N.K., A.S.N., A.M.M., A.M.Q., G.T.A. and A.V.S., writing—original draft preparation, V.G.N., A.G.T. and A.S.N.; writing—review and editing, V.G.N., A.G.T. and A.S.N. All authors have read and agreed to the published version of the manuscript.

Funding: This paper has been supported by the RUDN University Strategic Academic Leadership Program (award no. 025238-2-174, recipient: Tskhovrebov A.G.).

Data Availability Statement: Not applicable.

Conflicts of Interest: The authors declare no conflict of interest.

References

1. Nenajdenko, V.G.; Shastin, A.V.; Gorbachev, V.M.; Shorunov, S.V.; Muzalevskiy, V.M.; Lukianova, A.I.; Dorovatovskii, P.V.; Khrustalev, V.N. Copper-Catalyzed Transformation of Hydrazones into Halogenated Azabutadienes, Versatile Building Blocks for Organic Synthesis. *ACS Catal.* **2017**, *7*, 205–209. [CrossRef]
2. Nenajdenko, V.G.; Shastin, A.V.; Korotchenko, V.N.; Varseev, G.N.; Balenkova, E.S. A Novel Approach to 2-Chloro-2-fluorostyrenes. *Eur. J. Org. Chem.* **2003**, *2003*, 302–308. [CrossRef]
3. Shastin, A.V.; Muzalevsky, V.M.; Balenkova, E.S.; Nenajdenko, V.G. Stereoselective synthesis of 1-bromo-1-fluorostyrenes. *Mendeleev Commun.* **2006**, *16*, 179–180. [CrossRef]
4. Shastin, A.V.; Korotchenko, V.N.; Nenajdenko, V.G.; Balenkova, E.S. A Novel Synthesis of β,β-Dibromostyrenes. *Synthesis* **2001**, *2001*, 2081–2084. [CrossRef]
5. Nenajdenko, V.G.; Korotchenko, V.N.; Shastin, A.V.; Balenkova, E.S. Catalytic olefination of carbonyl compounds. A new versatile method for the synthesis of alkenes. *Russ. Chem. Bull.* **2004**, *53*, 1034–1064. [CrossRef]
6. Nenajdenko, V.G.; Muzalevskiy, V.M.; Shastin, A.V.; Balenkova, E.S.; Kondrashov, E.V.; Ushakov, I.A.; Rulev, A.Y. Fragmentation of Trifluoromethylated Alkenes and Acetylenes by N,N-Binucleophiles. Synthesis of Imidazolines or Imidazolidines (Oxazolidines) Controlled by Substituent. *J. Org. Chem.* **2010**, *75*, 5679–5688. [CrossRef]
7. Shixaliyev, N.Q.; Gurbanov, A.V.; Maharramov, A.M.; Mahmudov, K.T.; Kopylovich, M.N.; Martins, L.M.D.R.S.; Muzalevskiy, V.M.; Nenajdenko, V.G.; Pombeiro, A.J.L. Halogen-bonded tris(2,4-bis(trichloromethyl)-1,3,5-triazapentadienato)-M(iii) [M = Mn, Fe, Co] complexes and their catalytic activity in the peroxidative oxidation of 1-phenylethanol to acetophenone. *New J. Chem.* **2014**, *38*, 4807–4815. [CrossRef]
8. Shikhaliyev, N.Q.; Kuznetsov, M.L.; Maharramov, A.M.; Gurbanov, A.V.; Ahmadova, N.E.; Nenajdenko, V.G.; Mahmudov, K.T.; Pombeiro, A.J.L. Noncovalent interactions in the design of bis-azo dyes. *CrystEngComm* **2019**, *21*, 5032–5038. [CrossRef]
9. Beharry, A.A.; Woolley, G.A. Azobenzene photoswitches for biomolecules. *Chem. Soc. Rev.* **2011**, *40*, 4422–4437. [CrossRef]
10. Natansohn, A.; Rochon, P. Photoinduced Motions in Azo-Containing Polymers. *Chem. Rev.* **2002**, *102*, 4139–4176. [CrossRef]
11. Dsouza, R.N.; Pischel, U.; Nau, W.M. Fluorescent Dyes and Their Supramolecular Host/Guest Complexes with Macrocycles in Aqueous Solution. *Chem. Rev.* **2011**, *111*, 7941–7980. [CrossRef] [PubMed]
12. Nenajdenko, V.G.; Shikhaliyev, N.G.; Maharramov, A.M.; Atakishiyeva, G.T.; Niyazova, A.A.; Mammadova, N.A.; Novikov, A.S.; Buslov, I.V.; Khrustalev, V.N.; Tskhovrebov, A.G. Structural Organization of Dibromodiazadienes in the Crystal and Identification of Br·· O Halogen Bonding Involving the Nitro Group. *Molecules* **2022**, *27*, 5110. [CrossRef] [PubMed]
13. Shikhaliyev, N.G.; Maharramov, A.M.; Bagirova, K.N.; Suleymanova, G.T.; Tsyrenova, B.D.; Nenajdenko, V.G.; Novikov, A.S.; Khrustalev, V.N.; Tskhovrebov, A.G. Supramolecular organic frameworks derived from bromoaryl-substituted dichlorodiazabutadienes via Cl···Br halogen bonding. *Mendeleev Commun.* **2021**, *31*, 191–193. [CrossRef]

14. Nenajdenko, V.G.; Shikhaliyev, N.G.; Maharramov, A.M.; Bagirova, K.N.; Suleymanova, G.T.; Novikov, A.S.; Khrustalev, V.N.; Tskhovrebov, A.G. Halogenated Diazabutadiene Dyes: Synthesis, Structures, Supramolecular Features, and Theoretical Studies. *Molecules* **2020**, *25*, 5013. [CrossRef] [PubMed]
15. Shikhaliyev, N.G.; Maharramov, A.M.; Suleymanova, G.T.; Babazade, A.A.; Nenajdenko, V.G.; Khrustalev, V.N.; Novikov, A.S.; Tskhovrebov, A.G. Arylhydrazones of α-keto esters via methanolysis of dichlorodiazabutadienes: Synthesis and structural study. *Mendeleev Commun.* **2021**, *31*, 677–679. [CrossRef]
16. Wang, Y.-F.; Wang, C.-J.; Feng, Q.-Z.; Zhai, J.-J.; Qi, S.-S.; Zhong, A.-G.; Chu, M.-M.; Xu, D.-Q. Copper-catalyzed asymmetric 1,6-conjugate addition of in situ generated para-quinone methides with β-ketoesters. *Chem. Commun.* **2022**, *58*, 6653–6656. [CrossRef]
17. Yao, W.; Wang, J.; Lou, Y.; Wu, H.; Qi, X.; Yang, J.; Zhong, A. Chemoselective hydroborative reduction of nitro motifs using a transition-metal-free catalyst. *Org. Chem. Front.* **2021**, *8*, 4554–4559. [CrossRef]
18. Yao, W.; He, L.; Han, D.; Zhong, A. Sodium Triethylborohydride-Catalyzed Controlled Reduction of Unactivated Amides to Secondary or Tertiary Amines. *J. Org. Chem.* **2019**, *84*, 14627–14635. [CrossRef]
19. Bondi, A. Van der waals volumes and radii. *J. Phys. Chem.* **1964**, *68*, 441–451. [CrossRef]
20. Alvarez, S. A cartography of the van der Waals territories. *Dalt. Trans.* **2013**, *42*, 8617–8636. [CrossRef]
21. Tskhovrebov, A.G.; Novikov, A.S.; Kritchenkov, A.S.; Khrustalev, V.N.; Haukka, M. Attractive halogen···halogen interactions in crystal structure of trans-dibromogold(III) complex. *Z. Krist. Cryst. Mater.* **2020**, *235*, 477–480. [CrossRef]
22. Bader, R.F.W. A Quantum Theory of Molecular Structure and Its Applications. *Chem. Rev.* **1991**, *91*, 893–928. [CrossRef]
23. Bartashevich, E.V.; Tsirelson, V.G. Interplay between non-covalent interactions in complexes and crystals with halogen bonds. *Russ. Chem. Rev.* **2014**, *83*, 1181–1203. [CrossRef]
24. Usoltsev, A.N.; Sukhikh, T.S.; Novikov, A.S.; Shayapov, V.R.; Pishchur, D.P.; Korolkov, I.V.; Sakhapov, I.F.; Fedin, V.P.; Sokolov, M.N.; Adonin, S.A. Unexpected Polymorphism in Bromoantimonate(III) Complexes and Its Effect on Optical Properties. *Inorg. Chem.* **2021**, *60*, 2797–2804. [CrossRef]
25. Bolotin, D.S.; Il'in, M.V.; Suslonov, V.V.; Novikov, A.S. Symmetrical Noncovalent Interactions Br···Br Observed in Crystal Structure of Exotic Primary Peroxide. *Symmetry* **2020**, *12*, 637. [CrossRef]
26. Usoltsev, A.N.; Adonin, S.A.; Novikov, A.S.; Abramov, P.A.; Sokolov, M.N.; Fedin, V.P. Chlorotellurate(iv) supramolecular associates with "trapped" Br_2: Features of non-covalent halogen· · · halogen interactions in crystalline phases. *CrystEngComm* **2020**, *22*, 1985–1990. [CrossRef]
27. Adonin, S.A.; Bondarenko, M.A.; Novikov, A.S.; Abramov, P.A.; Plyusnin, P.E.; Sokolov, M.N.; Fedin, V.P. Antimony(V) Bromide and Polybromide Complexes with N-alkylated Quinolinium or Isoquinolinium Cations: Substituent-dependent Assembly of Polymeric Frameworks. *Z. Anorg. Allg. Chem.* **2019**, *645*, 1141–1145. [CrossRef]
28. Khrustalev, V.N.; Grishina, M.M.; Matsulevich, Z.V.; Lukiyanova, J.M.; Borisova, G.N.; Osmanov, V.K.; Novikov, A.S.; Kirichuk, A.A.; Borisov, A.V.; Solari, E.; et al. Novel cationic 1,2,4-selenadiazoles: Synthesis via addition of 2-pyridylselenyl halides to unactivated nitriles, structures and four-center Se···N contacts. *Dalt. Trans.* **2021**, *50*, 10689–10691. [CrossRef]
29. Chai, J.-D.; Head-Gordon, M. Long-range corrected hybrid density functionals with damped atom–atom dispersion corrections. *Phys. Chem. Chem. Phys.* **2008**, *10*, 6615–6620. [CrossRef]
30. Frisch, M.J.; Trucks, G.W.; Schlegel, H.B.; Scuseria, G.E.; Robb, M.A.; Cheeseman, J.R.; Scalmani, G.; Barone, V.; Mennucci, B.; Petersson, G.A.; et al. Gaussian09 Revision D.01. In *Gaussian 09 Revis. C.01*; Gaussian Inc.: Wallingford, CT, USA, 2010.
31. Marenich, A.V.; Cramer, C.J.; Truhlar, D.G. Universal Solvation Model Based on Solute Electron Density and on a Continuum Model of the Solvent Defined by the Bulk Dielectric Constant and Atomic Surface Tensions. *J. Phys. Chem. B* **2009**, *113*, 6378–6396. [CrossRef]
32. Lu, T.; Chen, F. Multiwfn: A multifunctional wavefunction analyzer. *J. Comput. Chem.* **2012**, *33*, 580–592. [CrossRef]
33. Tskhovrebov, A.G.; Novikov, A.S.; Tupertsev, B.S.; Nazarov, A.A.; Antonets, A.A.; Astafiev, A.A.; Kritchenkov, A.S.; Kubasov, A.S.; Nenajdenko, V.G.; Khrustalev, V.N. Azoimidazole Gold(III) Complexes: Synthesis, Structural Characterization and Self-Assembly in the Solid State. *Inorganica Chim. Acta* **2021**, *522*, 120373. [CrossRef]
34. Repina, O.V.; Novikov, A.S.; Khoroshilova, O.V.; Kritchenkov, A.S.; Vasin, A.A.; Tskhovrebov, A.G. Lasagna-like supramolecular polymers derived from the PdII osazone complexes via C(sp2)–H···Hal hydrogen bonding. *Inorganica Chim. Acta* **2020**, *502*, 119378. [CrossRef]
35. Astafiev, A.A.; Repina, O.V.; Tupertsev, B.S.; Nazarov, A.A.; Gonchar, M.R.; Vologzhanina, A.V.; Nenajdenko, V.G.; Kritchenkov, A.S.; Khrustalev, V.N.; Nadtochenko, V.N.; et al. Unprecedented Coordination-Induced Bright Red Emission from Group 12 Metal-Bound Triarylazoimidazoles. *Molecules* **2021**, *26*, 1739. [CrossRef]
36. Tskhovrebov, A.G.; Vasileva, A.A.; Goddard, R.; Riedel, T.; Dyson, P.J.; Mikhaylov, V.N.; Sorokoumov, V.N.; Haukka, M.; Serebryanskaya, T.V.; Sorokoumov, V.N.; et al. Palladium(II)-Stabilized Pyridine-2-Diazotates: Synthesis, Structural Characterization, and Cytotoxicity Studies. *Inorg. Chem.* **2018**, *57*, 930–934. [CrossRef]
37. Tskhovrebov, A.G.; Novikov, A.S.; Odintsova, O.V.; Mikhaylov, V.N.; Sorokoumov, V.N.; Serebryanskaya, T.V.; Starova, G.L. Supramolecular polymers derived from the PtII and PdII schiff base complexes via C(sp2)–H … Hal hydrogen bonding: Combined experimental and theoretical study. *J. Organomet. Chem.* **2019**, *886*, 71–75. [CrossRef]

38. Mikhaylov, V.N.; Sorokoumov, V.N.; Novikov, A.S.; Melnik, M.V.; Tskhovrebov, A.G.; Balova, I.A. Intramolecular hydrogen bonding stabilizes trans-configuration in a mixed carbene/isocyanide PdII complexes. *J. Organomet. Chem.* **2020**, *912*, 121174. [CrossRef]
39. Liu, Y.; Varava, P.; Fabrizio, A.; Eymann, L.Y.M.; Tskhovrebov, A.G.; Planes, O.M.; Solari, E.; Fadaei-Tirani, F.; Scopelliti, R.; Sienkiewicz, A.; et al. Synthesis of aminyl biradicals by base-induced Csp^3–Csp^3 coupling of cationic azo dyes. *Chem. Sci.* **2019**, *10*, 5719–5724. [CrossRef]
40. Bhorge, Y.R.; Chang, C.-T.; Chang, S.-H.; Yan, T.-H. $CHBr_3/TiCl_4/Mg$ as an Unusual Nucleophilic CBr_2 Carbenoid: Effective and Chemoselective Dibromomethylenation of Aldehydes and Ketones. *Eur. J. Org. Chem.* **2012**, *2012*, 4805–4810. [CrossRef]
41. Roper, K.A.; Berry, M.B.; Ley, S.V. The application of a monolithic triphenylphosphine reagent for conducting Ramirez gem-dibromoolefination reactions in flow. *Beilstein J. Org. Chem.* **2013**, *9*, 1781–1790. [CrossRef]
42. Bruker. *SAINT*; v. 8.34A; Bruker AXS Inc.: Madison, WI, USA, 2014.
43. Krause, L.; Herbst-Irmer, R.; Sheldrick, G.M.; Stalke, D. *SAINT* program. *Appl. Cryst.* **2015**, *48*, 3–10. [CrossRef] [PubMed]
44. Sheldrick, G.M. *SAINT* program. *Acta Cryst.* **2015**, *C71*, 3–8.